Electromagnetically induced transparency of single Λ-type three-level atoms in a high-finesse optical cavity*

Sun Yan-Fen(孙燕芬)[a], Tan Lei(谭 磊)[b]†, and Xu Yan(徐 岩)[c]

[a] Department of Physics, Lüliang University, Lüliang 033000, China
[b] Key Laboratory for Magnetism and Magnetic Materials of the Ministry of Education, Lanzhou University, Lanzhou 730000, China
[c] College of Science, Shandong University of Science and Technology, Qingdao 266510, China

(Received 6 July 2012; revised manuscript received 6 September 2012)

We study the features of electromagnetically induced transparency (EIT) in a single Λ-type three-level atom placed in a high-finesse cavity under the action of a coupling laser and a probe laser. Our calculations show that three transparency windows appear when the pump strength is large enough. This can be explained by the residual pump in the cavity mostly resulting in energy splitting. The level $|3\rangle$ is split into four slightly different energy levels, and interference takes place between the excitation pathways. Furthermore, it is also shown that the frequencies of the EIT windows can be tuned by changing the coupling field detuning Δ_2, and that the reflection profile is very sensitive to the cavity field detuning Δ_c.

Keywords: Λ-type three-level atom, high-finesse optical cavity, electromagnetically induced transparency

PACS: 03.65.Yz, 03.65.Ud, 03.67.Pp **DOI:** 10.1088/1674-1056/22/3/030309

1. Introduction

It is well known that electromagnetically induced transparency (EIT) is an interference effect in which the optical properties of a probe field are modified by the presence of a strong coupling field.[1] Practically, this is achieved by irradiating a medium with two laser beams. The action of a strong control laser causes the medium to become transparent for a weak probe laser. This phenomenon has been observed in a system of three-level atoms in the Λ configuration.[2] A large amount of literature on EIT now exists.[3–9] In addition, its wide applications, such as enhanced optical nonlinearity,[3,4] information storage,[5,6] and achieving an ultraslow group velocity of light,[7] have attracted considerable attention.

EIT has been a phenomenon specific to optically thick media consisting of ensembles of a very large number of atoms, where both the optical fields and the material states are modified. Recently, EIT with a single atom has been demonstrated.[10–12] In quantum optics, the presence of high-finesse cavities can be used to enhance photon–matter interaction. To scale down these systems to the single quantum level of matter and light, using high-finesse cavities[13] is the most studied route towards such a goal.[14] It represents a cornerstone in the development of new quantum-based information technologies, and these results are also fundamental for understanding how the quantum behavior of single atoms can be controlled by light.

Recently, Baur *et al*. observed Autler–Townes splitting in a three-level quantum system coupled to a cavity using the dispersive measurement.[15] The group velocity of a probe pulse in an ensemble of Λ-type atoms coupled to a quantized cavity mode depends on the quantum state of the input probe pulse.[16] EIT with a single atom quasi-permanently trapped inside a high-finesse optical cavity was demonstrated, and EIT scaling was investigated when the atom number was increased one by one.[10] None of these experiments studied multi-windows by using the three-level atoms in a cavity. In this paper, we will create three-window EIT by using a Λ-type three-level atom in a high-finesse optical cavity.

In the previous work, the multi-window EIT produced by multi-level schemes and the excitonic absorption in a semiconductor quantum well were demonstrated.[17–20] The role of EIT with a strong probe field and how multiple photon routes due to the presence of more than one driving field resulting in changes to the normal EIT absorption profile were investigated. In this paper, we investigate EIT with a single atom in an optical cavity using the master equation. In our model, we consider the dissipative processes of the system due to the interaction between the system and the environment, which include the leakage of photons from the cavity and the spontaneous emission from the atom. Scaling the medium down to a single atom, unlike that in an optical medium with atoms, the single atom EIT is revealed by the suppression of reflection of electromagnetic waves rather than the absorption.[11] In the strong coupling regime, a single photon is enough to saturate the atom in the cavity, and it dominates the dynamics of the system such that the interaction between the single

*Project supported by the National Natural Science Foundation of China (Grant Nos. 11274148 and 10704031), the Basic Scientific Research Business Expenses of the Central University, China (Grant No. lzujbky-2010-75), and the Open Project of Key Laboratory for Magnetism and Magnetic Materials of the Ministry of Education, Lanzhou University, China.

†Corresponding author. E-mail: tanlei@lzu.edu.cn

© 2013 Chinese Physical Society and IOP Publishing Ltd

atom and the photons can be manifestly nonlinear. Therefore, in our system, we assume that the average number of photons inside the cavity is no more than one. This assumption is reasonable because the typical average number of photons in a high-finesse optical cavity today is as low as 10^{-3}–10^{-4}.[21] We introduce the main features of the cavity EIT by means of reflection spectra and show how three transparency windows appear. In addition, the frequencies of the EIT windows can be tuned by changing the detuning Δ_2, and rich phenomena are found when the cavity field detuning $|\Delta_c|$ reaches some finite values.

This paper is organized as follows. In Section 2, we briefly describe the EIT model with an atom inside an optical cavity and derive the motion equations for the density matrix of the system. In Section 3, we investigate how three transparency windows appear. The effects of coupling field detuning and cavity field detuning on cavity EIT are also studied. Finally, a brief conclusion is given in Section 4.

2. Model and motion equation

The driven atom–cavity configuration and the atomic energy level scheme are shown schematically in Fig. 1. In Fig. 1(a), a single three-level atom is trapped in a high-finesse cavity with the decay constant κ. The cavity is driven by a coherent laser which couples to the cavity with a strength η. An additional laser directly couples to the atomic transition with the Rabi frequency Ω_c. In Fig. 1(b), a Λ-type three-level atom consisting of an excited state $|3\rangle$ coupled to the atomic ground state $|1\rangle$ by the single quantized cavity mode of frequency ω_{cav} is shown. A strong coupling laser with frequency ω_c near the ω_2 resonance couples levels $|2\rangle$ and $|3\rangle$. The atomic transition $|1\rangle \leftrightarrow |2\rangle$ is dipole forbidden. With rotating wave approximation, the master equation for the density-matrix operator ρ of the system can be given as[22]

$$\dot{\rho} = -\frac{\mathrm{i}}{\hbar}[H_{ac} + H_p, \rho] + L_a\rho + L_c\rho, \tag{1}$$

where

$$\begin{aligned} H_{ac} &= \hbar\Delta_1 A_{11} + \hbar\Delta_2 A_{22} - \hbar\Delta_c a^\dagger a + \hbar g_1(\mathbf{r})(a^\dagger A_{13} + A_{31} a) \\ &\quad + \hbar\Omega_c(A_{23} + A_{32}), \qquad (2) \\ H_p &= \mathrm{i}\hbar\eta(a^\dagger - a), \qquad (3) \\ L_c\rho &= \kappa(2a\rho a^\dagger - a^\dagger a\rho - \rho a^\dagger a), \qquad (4) \\ L_a\rho &= \gamma_2(2A_{13}\rho A_{31} - \rho A_{33} - A_{33}\rho) \\ &\quad + \gamma_3(2A_{23}\rho A_{32} - \rho A_{33} - A_{33}\rho), \qquad (5) \end{aligned}$$

with atomic detunings $\Delta_1 = \omega_p - \omega_1$, $\Delta_2 = \omega_c - \omega_2$, and cavity detuning $\Delta_c = \omega_p - \omega_{cav}$. Here, H_{ac} stands for the interaction between the atom and the cavity fields, and H_p is the pump field Hamiltonian. The cavity mode is described by the creation and annihilation operators $a^\dagger$ and a, while the atom is represented by the operator $A_{ij} = |i\rangle\langle j|$ $(i, j = 1, 2, 3)$. $g_1(\mathbf{r})$ is the coupling strength between the atom and the cavity field associated with the atomic transition $|1\rangle \leftrightarrow |3\rangle$, and Ω_c is the Rabi frequency related to the atomic transition $|2\rangle \leftrightarrow |3\rangle$. L_c and L_a, respectively, describe the decay of the resonator mode and the atomic damping to the background modes, and γ_2 and γ_3 are the decay rates of $|3\rangle \to |1\rangle$ and $|3\rangle \to |2\rangle$, respectively. We assume that the cavity is very weakly driven. In this case, the operator products factorized for the steady state of a motionless atom are written as[22] $\langle aA_{ij}\rangle = \langle a\rangle\langle A_{ij}\rangle, \langle a^\dagger A_{ij}\rangle = \langle a^\dagger\rangle\langle A_{ij}\rangle$. By using Eqs. (1) and (5), the dynamical equations for the expectation values $\langle A_{ij}\rangle$ and $\langle a\rangle$ can be written as

$$\begin{aligned} \langle\dot{a}\rangle &= \mathrm{i}\Delta_c\langle a\rangle - \mathrm{i}g_1\langle A_{13}\rangle - \kappa\langle a\rangle + \eta, \qquad (6) \\ \langle\dot{A_{11}}\rangle &= -\mathrm{i}g_1\langle a^\dagger\rangle\langle A_{13}\rangle + \mathrm{i}g_1\langle a\rangle\langle A_{31}\rangle + 2\gamma_2\langle A_{33}\rangle, \qquad (7) \\ \langle\dot{A_{22}}\rangle &= -\mathrm{i}\Omega_c\langle A_{23}\rangle + \mathrm{i}\Omega_c\langle A_{32}\rangle + 2\gamma_3\langle A_{33}\rangle, \qquad (8) \\ \langle\dot{A_{12}}\rangle &= \mathrm{i}(\Delta_1 - \Delta_2)\langle A_{12}\rangle + \mathrm{i}g_1\langle a\rangle\langle A_{32}\rangle - \mathrm{i}\Omega_c\langle A_{13}\rangle, \qquad (9) \\ \langle\dot{A_{13}}\rangle &= \mathrm{i}\Delta_1\langle A_{13}\rangle - \mathrm{i}g_1\langle a\rangle\langle(A_{11} - A_{33})\rangle \\ &\quad - \mathrm{i}\Omega_c\langle A_{12}\rangle - (\gamma_2 + \gamma_3)\langle A_{13}\rangle, \qquad (10) \\ \langle\dot{A_{23}}\rangle &= \mathrm{i}\Delta_2\langle A_{23}\rangle - \mathrm{i}\Omega_c\langle(A_{22} - A_{33})\rangle \\ &\quad - \mathrm{i}g_1\langle a\rangle\langle A_{21}\rangle - (\gamma_2 + \gamma_3)\langle A_{23}\rangle. \qquad (11) \end{aligned}$$

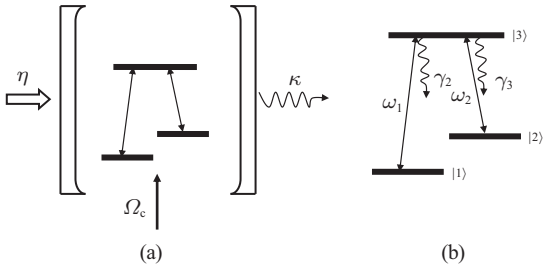


Fig. 1. (a) A single three-level atom trapped in an optical cavity with the decay constant κ. The cavity is driven by a coherent laser, which couples to the cavity mode with strength η. An additional laser with Rabi frequency Ω_c is directly coupled to the atomic transition. (b) The atomic energy level scheme.

The atomic operator $A_{ij} = |i\rangle\langle j|$ satisfies the commutator relation $[A_{ij}, A_{kl}] = A_{il}\delta_{jk} - A_{kj}\delta_{il}$ and the condition $\langle A_{11}\rangle + \langle A_{22}\rangle + \langle A_{33}\rangle = 1$. The expectation value $\langle a\rangle$ given in Eq. (6) depends mostly on the pump strength η. As η increases, the effect of the quantized field becomes prominent. We are then likely to get some new features. We consider all the elements of the reduced density operator of the atom, the field operators of the cavity mode, and the evolution equations for the averages of these variables. Analytical solutions to the master equations (6)–(11) are very complicated, but the steady solutions can be obtained. In solving the master equation for the atom–cavity system, we take the routine steady solution method, assuming that all the density matrix elements of the system do not evolve with time in the long run.

3. Three transparency windows

The electromagnetic response of a single atom is naturally characterized by polarizability α. The atom scatters waves, and the polarizability is related to the reflection according to $\alpha \propto \mathrm{i}r$,[23] where r is the reflection coefficient. For a natural atom, we can define the polarizability $\alpha = \alpha' + \mathrm{i}\alpha''$. The polarization components can be obtained in terms of the density matrix element ρ_{31} by $\alpha = 2N\mu_{13}\rho_{31}$,[24] where $\langle A_{ij}\rangle = \mathrm{Tr}[A_{ij}\rho] = \rho_{ji}$ and N is the atomic density. For the sake of simplicity, we assume $2N\mu_{13} = 1$, so we have α=ρ_{31}. In the vicinity of the resonance, we have

$$\mathrm{Re}(r) \propto \alpha'', \tag{12}$$

$$\mathrm{Im}(r) \propto -\alpha'. \tag{13}$$

Therefore, the dispersion and the reflection are determined by α and related to the real and the imaginary parts α' and α'', respectively.

The master equations (6)–(11) are solved numerically. A numerical result of the reflection can be found in Fig. 2. It can be seen that the reflection vanishes at the probe resonance, which demonstrates the EIT effect. At the same time, the linewidth of the transparency window (the full width of the EIT resonance at half maximum) is the Rabi frequency of the coupling field Ω_c, which can be explained by the dressed state.[25] The Autler–Townes splitting arises due to the Rabi splitting of level $|3\rangle$ under the strong drive.[26]

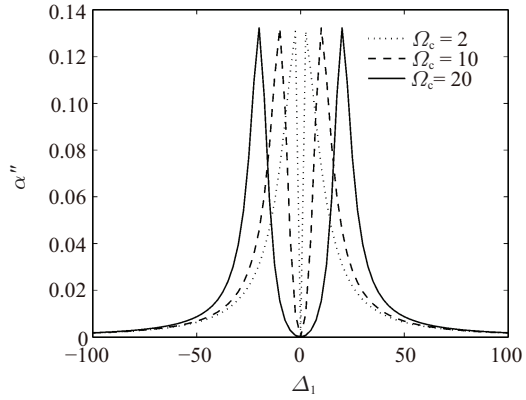


Fig. 2. Variations of α'' vs detuning Δ_1 for different coupling strengths between the atom and the control field Ω_c. The parameters are set to $(g_1, \eta, \kappa, \gamma_2, \gamma_3, \Delta_c, \Delta_2) = 2\pi \times (3, 0.5, 1, 1, 1, 0, 0)$ MHz.

There is an interesting feature in this atom–cavity system. It is possible to create a three-window EIT in such a system, as shown in Fig. 3, and it can be found that the probe photons are strongly reflected at frequencies $\Delta_1 = \pm\Omega_c$ when the pump strength is small. When η is large enough, we observe that the two peaks (at frequencies $\Delta_1 = \pm\Omega_c$) shown for the case $\eta = 0.5$ MHz develop into a double peak (see the plot for $\eta = 2.0$ MHz). In Fig. 4, we plot α'' for different detunings. One of the peaks is for an observation frequency $\Delta_1 > \Omega_c$ and has a height larger than that of the other peak for $\Delta_1 < \Omega_c$. With the enhanced pump strength, we obtain a deeper and broader transparency dip. Although the essential multi-window EIT physics have been well understood from the studies of complicated multi-level systems,[17] there are three-window EITs in simple three-level systems. It should be noted that changing the pump strength η changes the spectral profile of the reflection, and three transparency windows appear as η is increased. This can be explained by the residual pump in the cavity resulting mostly in the pump field and the atom coupling, which causes energy splitting. Energy level $|3\rangle$ splits into a pair of states in the presence of a strong coupling field, and the pair of levels are split by the residual pump again. It can been seen from Fig. 5 that the level $|3\rangle$ (dotted line) splits in the presence of a strong coupling field, and the energy eigenvalues (dashed line) are[19]

$$E_{+,n} = \hbar\omega_{\mathrm{cav}} - \frac{\hbar}{2}\Delta_1 + \frac{\hbar}{2}\sqrt{4\Omega_c^2 + \Delta_1^2}, \tag{14}$$

$$E_{-,n} = \hbar\omega_{\mathrm{cav}} - \frac{\hbar}{2}\Delta_1 - \frac{\hbar}{2}\sqrt{4\Omega_c^2 + \Delta_1^2}. \tag{15}$$

The coupling-induced shift in energy levels is $E_{+,n} - E_{-,n} = 2\Omega_c$ for $\Delta_1 = 0$ and $\hbar = 1$. With the increase in the pump strength η, the coupling strength between the atom and the cavity field monotonically increases, and the pair of levels split again. Level $|3\rangle$ is split into four slightly different energy levels (the solid line in Fig. 5). An interference between the excitation pathways then occurs. The probabilities for the system to transfer between levels can interfere destructively, preventing reflection. In Fig. 5, we notice that the linewidth of the EIT is approximately proportional to $g(r)$.

We now discuss the effect of the detuning of the coupling field Δ_2 on the EIT from two aspects: the reflection and the population. In Fig. 6, we plot the imaginary part of polarizability α'' as a function of the probe detuning from atomic transition resonance Δ_1 for different detuning Δ_2. When $\Delta_2 = 0$, the minimum position for reflection is at $\Delta_1 = 0$. However, when $\Delta_2 \neq 0$, the minimum frequency is shifted to $\Delta_1 = \Delta_2$

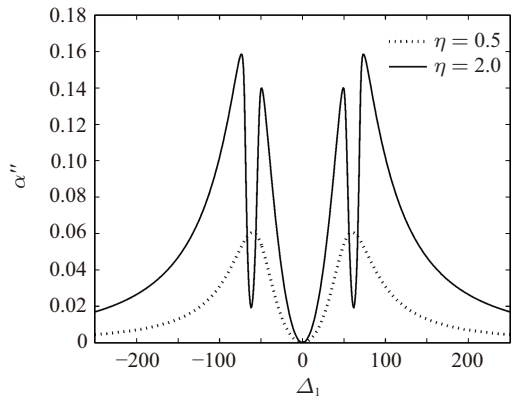


Fig. 3. Variations of α'' vs detuning Δ_1 for different pump strengths, η. The parameters are set to $(g_1, \Omega_c, \kappa, \gamma_2, \gamma_3, \Delta_c, \Delta_2) = 2\pi \times (8, 60, 1, 1, 1, 0, 0)$ MHz.

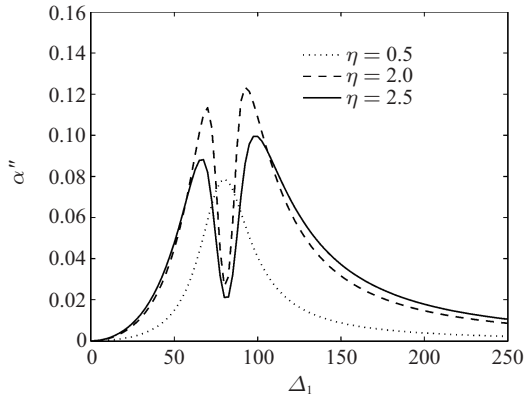


Fig. 4. Variations of α'' vs detuning Δ_1 for different pump strengths, η. The parameters are set to $(g_1, \Omega_c, \kappa, \gamma_2, \gamma_3, \Delta_c, \Delta_2) = 2\pi \times (6, 80, 1, 1, 1, 0, 0)$ MHz.

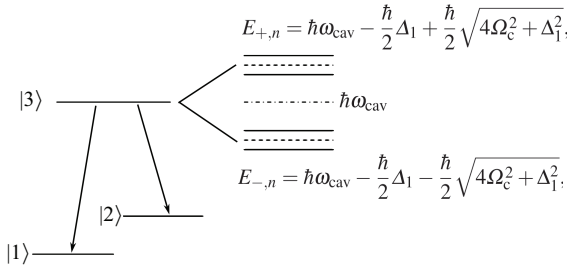


Fig. 5. The dressed states of the coupled atom and strong coupling field. Level $|3\rangle$ is split into four slightly different energy levels (solid line).

(dashed line), which shows that the transparency windows shift as Δ_2. This is in agreement with the single atom EIT effect.[10] Mücke and his colleagues showed that the transparency window appearing at the two-photon resonance can be shifted by changing the control-laser frequency. We have $\Delta_2 = \Delta_1$ and $\Delta_1 = \omega_{cav} - \omega_1$, so photons with frequency $\omega_{cav} = \omega_1 + \Delta_2$ are likely to transmit through the cavity. The frequencies of the EIT windows can also be tuned by changing Δ_2. At the same time, the reflection profile becomes highly asymmetric when $\Delta_2 \neq 0$. We discuss the dressed-state interpretation. The level $|3\rangle$ is shifted up and down by an amount $\hbar\omega^{\pm} = (\Delta_1 \pm \sqrt{\Omega_c^2 + \Delta_1^2})\hbar/2$ at the strong drive.[19] As shown in Fig. 6, as $|\Delta_1|$ increases, one of the doublet peaks closes to the central frequency ($\Delta_1 = 0$), and its transparency window gets deeper. However, the other doublet peak gradually moves away from the central frequency, and the depth of the transparency window also diminishes. Furthermore, we plot $\rho_{11} + \rho_{22}$, the total population of levels $|1\rangle$ and $|2\rangle$, which also describes the transmission of photons through the cavity. When $\Delta_1 = 0$, we find that the population in these two lower levels is indeed 1. This corresponds to the solid curve of $\alpha''(\Delta_1)$ in Fig. 7. When $\Delta_2 = 20$ MHz, the position of the maximum is at $\Delta_1 = 20$ MHz, whereas it is at $\Delta_1 = -20$ MHz when $\Delta_2 = -20$ MHz. Thus, the imaginary part of polarizability α and the total population of the lower levels of the single Λ-type three-level atom give essentially the same result.

We now believe that we can obtain a shifted EIT window by controlling the detuning between the frequency of the strong coherent field ω_c and the atomic resonance between levels $|3\rangle$ and $|2\rangle$.

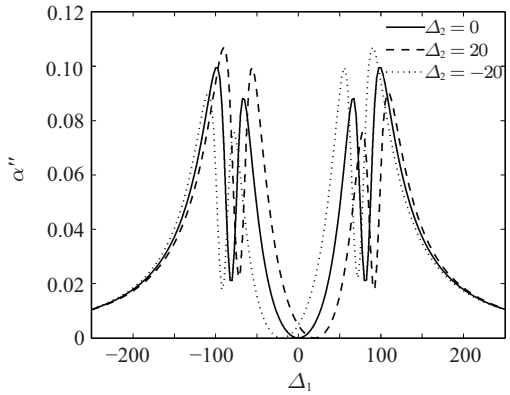


Fig. 6. Variations of α'' vs detuning Δ_1 for different coupling field detunings, Δ_2. The parameters are set to $(g_1, \Omega_c, \eta, \kappa, \gamma_2, \gamma_3, \Delta_c) = 2\pi \times (6, 80, 2.5, 1, 1, 1, 0)$ MHz.

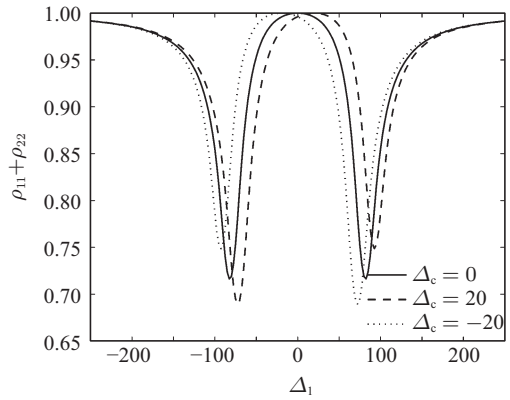


Fig. 7. Variations of population $\rho_{11} + \rho_{22}$ vs detuning Δ_1 for different coupling field detunings, Δ_2. The parameters are set to $(g_1, \Omega_c, \eta, \kappa, \gamma_2, \gamma_3, \Delta_c) = 2\pi \times (6, 80, 2.5, 1, 1, 1, 0)$ MHz.

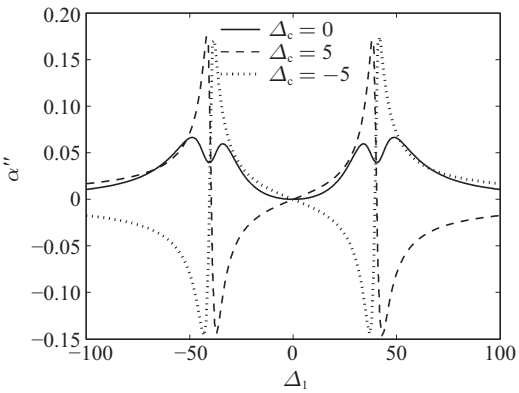


Fig. 8. Variations of α'' vs detuning Δ_1 for different cavity field detunings, Δ_c. The parameters are set to $(g_1, \Omega_c, \eta, \kappa, \gamma_2, \gamma_3, \Delta_2) = 2\pi \times (3, 40, 2.5, 1, 1, 1, 0)$ MHz.

Finally, we emphasize the sensitivity of α'' to the cavity field detuning Δ_c. In Fig. 8, it is found that α'' is very sensitive. For the case of $\Delta_c = 0$, the perfect EIT has been obtained.

However, when $|\Delta_c|$ is big enough, the spectral profile of reflection is changed strongly. For the case of $\Delta_c = 5$ MHz, at frequencies $\Delta_1 \in [-\Omega_c, 0]$ and $\Delta_1 \in [\Omega_c, +\infty]$, $\alpha'' < 0$. For cavity detuning $\Delta_c = -5$ MHz, we find a similar behavior at frequencies $\Delta_1 \in [0, \Omega_c]$ and $\Delta_1 \in [-\infty, -\Omega_c]$. These behaviors are similar to the gain of absorption,[27] and the effect of cavity EIT becomes diverse by changing Δ_c.

4. Conclusion

In this paper, we studied the EIT features of a single atom-cavity system. We described the main features of the cavity EIT by means of reflection spectra, and first found the dependence of the width of the EIT window on the coupling field strength. Our results showed that a Λ-type three-level atom placed in a high-finesse cavity shows three transparency windows when the pump strength η is big enough compared to the leakage rate of the photons from the cavity. At the same time, the frequencies of the cavity EIT can be controlled by changing the coupling field detuning Δ_2. Furthermore, it was found that α'' is very sensitive to cavity field detuning Δ_c. When Δ_c is large enough, the reflection has the effect of the gain $\alpha'' < 0$.

References

[1] Harris S E 1997 *Phys. Today* **50** 36
[2] Marangos J P 1998 *J. Mod. Opt.* **45** 471
[3] Dorman C, Kucukkara I and Marangos J P 1999 *Phys. Rev. A* **61** 013802
[4] Kang H S, Hernandez G and Zhu Y F 2005 *J. Mod. Opt.* **52** 2391
[5] Fleischhauer M and Lukin M D 2000 *Phys. Rev. Lett.* **84** 5094
[6] Raczynski A and Zaremba J 2002 *Opt. Commun.* **209** 149
[7] Zhang J P, Hernandez G and Zhu Y F 2008 *Opt. Lett.* **33** 46
[8] Yang B D, Gao J, Liang Q B, Wang J, Zhang T C and Wang J M 2011 *Chin. Phys. B* **20** 044202
[9] Niu J Y, Pei L Y, Wu L A and Fu P M 2010 *Chin. Phys. B* **19** 113209
[10] Mücke M, Figueroa E, Bochmann J, Hahn C, Murr K, Ritter S, Villas-Boasz C J and Remp G 2010 *Nature* **465** 699
[11] Abdumalikov A A, Astafiev O, Zagoskin A M, Pashkin Yu A, Nakamura Y and Tsai J S 2010 *Phys. Rev. Lett.* **104** 193601
[12] Kampschulte T, Alt W, Brakhane S, Eckstein M, Reimann R, Widera A and Meschede D 2010 *Phys. Rev. Lett.* **105** 153603
[13] Khudaverdyan M, Alt W, Dotsenko I, Kampschulte T, Lenhard K, Rauschenbeutel A, Reick S, Schörner K, Widera A and Meschede D 2008 *New J. Phys.* **10** 073023
[14] Imamoğlu A, Schmidt H, Woods G and Deutsch M 1997 *Phys. Rev. Lett.* **79** 1467
[15] Baur M, Filipp S, Bianchetti R, Fink J M, Göppl M, Steffen L, Leek P J, Blais A and Wallraff A 2009 *Phys. Rev. Lett.* **102** 243602
[16] Nikoghosyan G and Fleischhauer M 2010 *Phys. Rev. Lett.* **105** 013601
[17] McGloin D, Fulton D J and Dunn M H 2001 *Opt. Commun.* **190** 221
[18] Wang J, Kong L B, Jiang K J, Xiong H W, Zhu Y F and Zhan M S 2004 *Phys. Lett. A* **328** 437
[19] Li S J, Yang X D, Cao X M, Xie Ch D and Wang H 2007 *J. Phys. B: At. Mol. Opt. Phys.* **40** 3211
[20] Wu H W and Mi X W 2012 *Chin. Phys. B* **21** 107102
[21] Ruiller, Northup T E, Birnbaum K M, Boca A, Boozer A D and Kimble H J 2005 *J. Phys. B: At. Mol. Opt. Phys.* **38** S551
[22] Rebi S, Gangl M, Horak P and Ritsch H 1998 *Phys. Rev. A* **58** 3030
[23] Astafiev O, Zagoskin A M, Abdumalikov A A, Pashkin Yu A, Yamamoto T, Inomata K, Nakamura Y and Tsai J S 2010 *Science* **327** 840
[24] Scully M O and Zubairy M S 1997 *Quantum Optics* (Cambridge: Cambridge University Press)
[25] Fleischhauer M 2005 *Rev. Mod. Phys.* **77** 633
[26] Li Zh H, Li Y, Dou Y F and Zhang J X 2012 *Chin. Phys. B* **21** 034204
[27] Wu Y and Yang X X 2005 *Phys. Rev. A* **71** 053806